International Journal of Chemical, Materials and Biomolecular Sciences
ISSN: 2415-6620
Vol:10, No:8, 2016

Effect of Laser Input Energy on the Laser Joining of Polyethylene Terephthalate to Titanium

Y. J. Chen, T. M. Yue, Z. N. Guo

***Abstract*—**This paper reports the effects of laser energy on the characteristics of bubbles generated in the weld zone and the formation of new chemical bonds at the Polyethylene Terephthalate (PET)/Ti joint interface in laser joining of PET to Ti. The samples were produced by using different laser energies ranging from 1.5 J – 6 J in steps of 1.5 J, while all other joining parameters remained unchanged. The types of chemical bonding at the joint interface were analysed by the x-ray photoelectron spectroscopy (XPS) depth-profiling method. The results show that the characteristics of the bubbles and the thickness of the chemically bonded interface, which contains the laser generated bonds of Ti–C and Ti–O, increase markedly with increasing laser energy input. The tensile failure load of the joint depends on the combined effect of the amount and distribution of the bubbles formed and the chemical bonding intensity of the joint interface.

***Keywords*—**Laser direct joining, Ti/PET interface, laser energy, XPS depth profiling, chemical bond, tensile failure load.

I. Introduction

IN recent years, the demand of integrating different materials, such as light metals and plastics, is obvious and mainly necessary because of resource, energy, and environmental concerns. Since Gower et al. [1] successfully achieved the laser joining of a metal to a polymer, the revolutionary technique used has received considerable attention. The mechanism of laser joining of metals and plastics was first studied by Katayama and Kawahito [2], who named the joining technique laser-assisted metal and plastic (LAMP) joining. This technique has since been employed to create strong joints between engineering metals (e.g., stainless steel, Mg, and aluminum alloys) and plastics (e.g., PET and cyclic olefin polymers) by using a near-Gaussian laser beam or a line-shaped laser beam [2]-[5].

In LAMP, the transmission of the laser beams through the plastic leads to a relatively high temperature increase at the interface between the metal and plastic materials. As a result, the plastic in the weld zone is melted, and decomposition occurs, causing the formation of small bubbles in the molten plastic. After the molten plastic has cooled, an adhesive bond is formed between the metal and the plastic. Wahba et al. [3] partly attributed the strong bond formed between the metal and plastic material to the formation of bubbles in the molten plastic during laser irradiation. They hypothesised that the laser-induced bubbles induce high pressure in the molten plastic forcing it to come into close contact with the metal surface. As a result, the molten plastic enters the concavities, producing anchoring effects.

Yujiao Chen is with the Hong Kong Polytechnic University, Hong Kong (e-mail: 13902125r@connect.polyu.hk).

The chemical bonds created between the metal and plastic material at the joint interface have also been recognised as contributing to the overall joint strength. Research groups at Wayne State University and Fraunhofer Center for Laser Technology studied the interfacial bonding in Ti-coated glass/polyimide (TiG/PI) and Ti/PI pairs [6]-[9]. They found that the failure of the Ti/PI joint occurred within the PI, whereas for the TiG/PI joint, the fracture occurred in the glass substrate [7]. This result implies that in both cases, the PI was firmly bonded to the Ti surface due to the generation of strong chemical bonds [7]. The evidence of the formation of new chemical bonds during the LAMP joining of metals to plastics were also studied by Arai et al. [5], and Georgiev et al. [10], [11], who reported the formation of Ti–F and Ti–O bonds in the joining of Teflon FEP to Ti. Sano et al. [12] also reported a strong joint strength between Cu and PET due to the generation of new chemical bonds between Cu and O of PET.

The strong bonds reported in the aforementioned studies are attributed to close contact between the metal and plastic parts, resulting in the formation of chemical bonds. However, studies on the laser processing factors that influence the generation of beneficial chemical bonds are still lacking. With this in mind, this study employs XPS depth-profiling analysis to investigate the effect of laser energy on the nature of chemical bonding of the Ti/PET interface. In addition, the laser energy effect on the characteristics of the bubbles formed in the joint is studied. It is envisaged that the characteristics of the bubbles and the chemical bonds would have notable effects on the failure load of the joint.

II. Materials and Methods

A. Materials and Setup

The materials used in this study were Ti sheets (purity 99.6%) and PET sheets (amorphous) purchased from the Goodfellow Corporation. The sheet dimensions were 60 × 20 × 1 mm. Prior to laser welding, the Ti sheets were polished using #800, #1200, #1500, and #2000 emery paper, cleaned in an ultrasonic bath for 10 min in ethanol and then dried at 60 °C for 2 h.

Laser joining of PET to Ti was performed using a pulsed Nd: YAG laser (wavelength was 1064 nm) with a fibre-optic beam delivery system, which has a maximum average output power of 300 W. The laser spot size was 3 mm, and a welding speed of 4 mm/s and a laser frequency of 20 Hz were used. A transmission joining configuration of LAMP together with the dimensions of the specimen are shown in Fig. 1. During the joining process, the laser beam passed through a fixed top quartz glass and the PET sheet, which has a transmittance of 92% at $\lambda = 1064$ nm, before reaching the surface of the Ti sheet.

Four PET/Ti joints were produced by using different laser energies: Sample 1 (1.5 J), Sample 2 (3 J), Sample 3 (4.5 J), and Sample 4 (6 J).

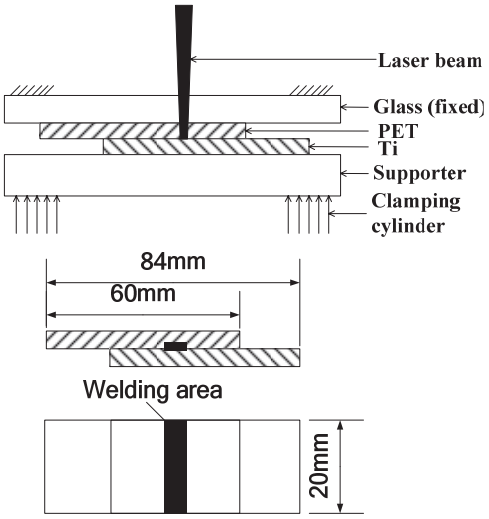

Fig. 1 A schematic diagram showing the transmission joining configuration of the Ti-PET pair

B. XPS Analysis

XPS was utilized to obtain information on the chemical bonds of the Ti/PET interface. For the XPS analysis, the Ti/PET joined samples were separated at the interface by means of a shear test, and analysis was performed on the Ti part at the center point of the joint. To reveal the nature of the chemical bonding across the interface, ion milling was used to gradually thin the solidified PET layer till reaching the Ti substrate.

After fracture, the Ti side of the sample was immediately placed into the UHV chamber (pressure = 10^{-6} Pa) of the XPS analyzer (ULVAC-PHI 1800) with an achromatic Al Kα X-ray source. Low-resolution spectra were recorded by using pass energy of 187.85 eV; for high-resolution spectra, the pass energy was 58.7 eV. The analysis was conducted in a semi-quantitative mode, and the XPS data were fitted by using the curve-fitting program of the XPSPEAK software.

III. Results and Discussion

A. Joint Appearance

Fig. 2 shows the joint appearance as a function of laser energy. For Sample 1 which was processed using laser energy of 1.5 J, no porosity was observed in the joint. It was found that if laser energy higher than 1.5 J was used, a large amount of bubbles developed in the weld zone. The development of bubbles is due to excessive laser energy causing decomposition of the polymer. It was noticed that the distribution of bubbles also altered as the laser energy was increased. It was observed that when relatively low laser energy was used, most of the bubbles were formed along the centerline of the weld where the laser energy was concentrated, and the bubbles appear in a somewhat discrete manner (Sample 2). When the laser energy increases, more bubbles were produced and they would agglomerate and were connected (Sample 3). However, when the laser energy was further increased, the bubbles become somewhat broken up (Sample 4). This could be due to the violent decomposition effect that occurs at high laser energies, causing the broken up of the bubbles.

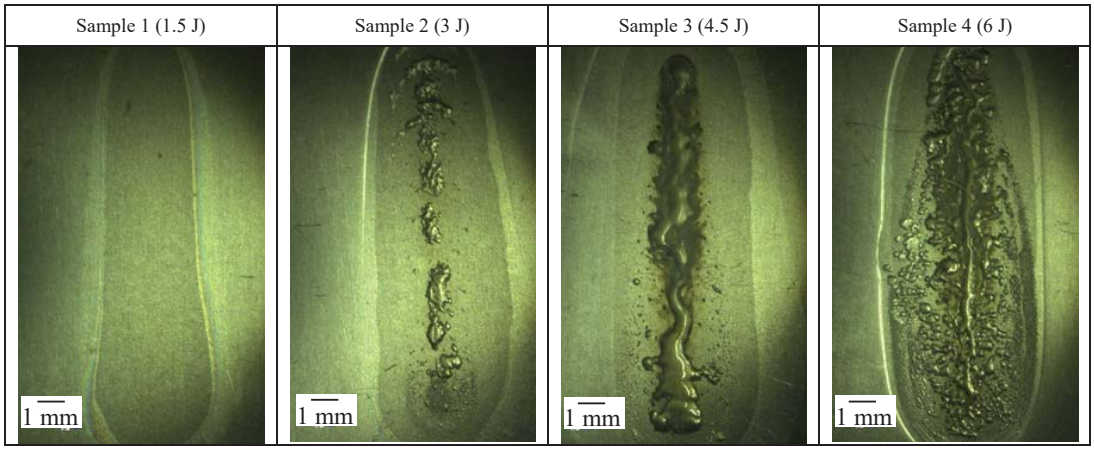

Fig. 2 Typical joint appearances as a function of laser power

B. XPS Analysis

1. C1s XPS Spectra

Fig. 3 shows a typical high-resolution XPS spectrum of the C1s lines of a laser joined sample which was ion milled to a depth just before reaching the chemically reacted PET/Ti interface zone (designated d=0). The C1s peak at ~284.8 eV, likely caused by the C–C bond [13], [14], and the peaks at approximately 286.6 eV and 289.2 eV correspond to –O–CH_2– and –C=O which originate from the PET chain [14]. No new peaks could be found, which suggests that some residual PET covered the Ti side after mechanical separation.

Fig. 4 shows the high-resolution C1s XPS spectra obtained

from the Ti side of the four joined samples, welded by using different laser energies after further ion-milling from (d=0) to different depths across the Ti/PET interface. After ion-milling to a further depth of 60 nm, a new weak peak at a binding energy of ~281.7 eV, likely to be the Ti–C bond [13], appeared in the spectra of the four samples. Mian [9] discovered that Ti atoms reacted with both five and six-fold rings of polyimide when laser welding polyimide to Ti sheets. Therefore, it is likely that titanium atoms can react with the phenyl carbons from the PET, just as in the case of polyimide/Ti produced by laser joining [9]. The areas of the C–C and Ti–C peaks decreased with increasing ion milling depth (Fig. 4). The peaks at 284.8 eV and 281.7 eV disappeared at sputtering depths of 480 nm and 750 nm, respectively (Fig. 4 (a)). This suggests that the thickness of the interface containing the laser generated Ti–C bonds is between 720 nm and 750 nm. The data shown in Fig. 4 indicate that the thickness of the interface containing the new Ti–C chemical bond is ~1200 nm in Sample 2, ~1500 nm in Sample 3, and ~1700 nm in Sample 4. This indicates that more Ti atoms react with the phenyl carbons when the laser input energy is increased. Fig. 5 shows the relationship between laser energy and the estimated Ti-C boned interface thickness.

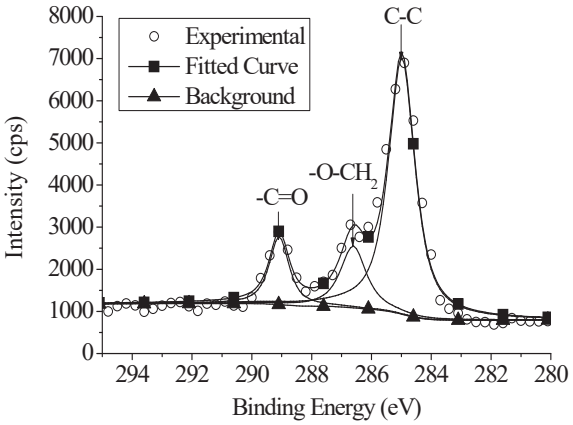

Fig. 3 Curve fitting of the C1s high resolution XPS spectra obtained from the Ti side of a laser joined sample

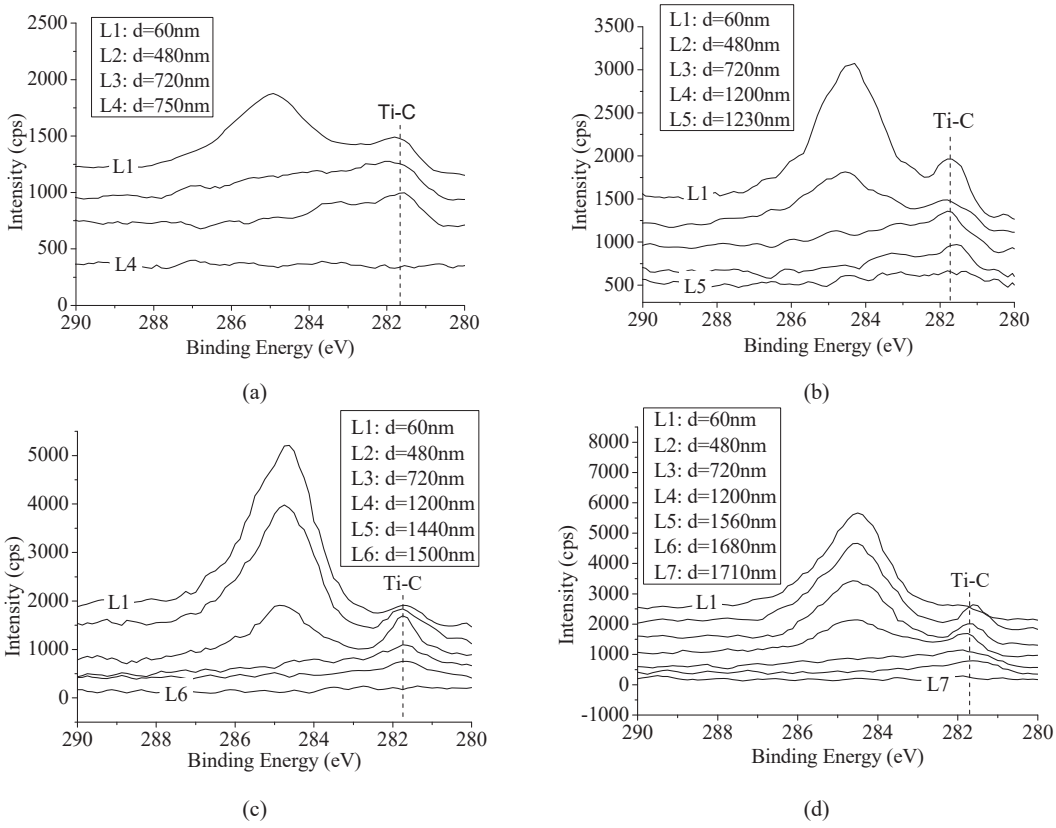

Fig. 4 High resolution of C1s XPS spectra obtained from the Ti side of the joined samples: (a) sample 1, (b) sample 2, (c) sample 3, (d) sample 4

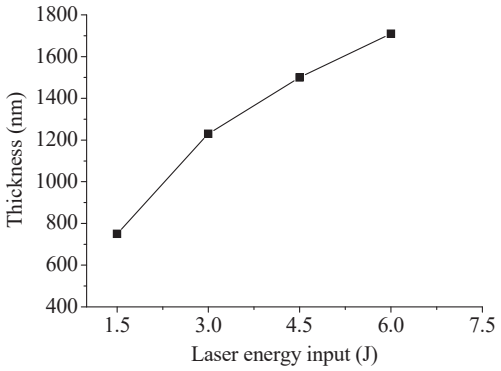

Fig. 5 The relationship between the laser energy input and the thickness of the interface containing the chemical bond of Ti-C

2. Ti2p XPS Spectra

Fig. 6 shows the high-resolution Ti2p XPS spectra of the four samples at various sputtering depths (measuring from d=0). Some new chemical bonds (e.g., Ti–C, Ti–O and Ti2O3) were formed in the joining process. At d=0, only the TiO2 peak with a Ti2p3/2 binding energy of 459.3 eV was present, this phase is believed to be the naturally formed oxide at the Ti surface. After further ion milling to a depth 60 nm, a broad binding energy peak (453.7–456.5 eV) was obtained, which can be attributed to the formation of new Ti–C, Ti–O and Ti2O3 bonds. The peaks at 454.8 eV, 455.1 eV, and 456.8 eV were most likely due to the Ti–C bond [13], the Ti–O bond [13] and the formation of Ti_2O_3 [15], respectively.

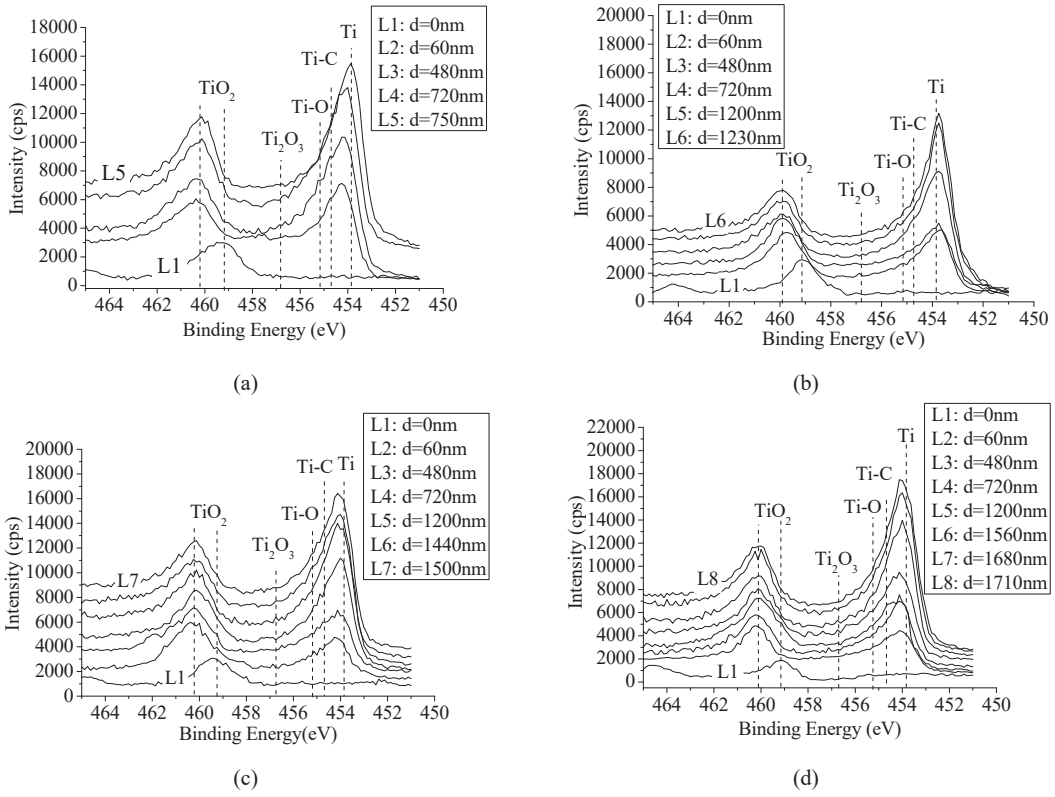

Fig. 6 High resolution of Ti2p XPS spectra taken from the Ti side of the joined samples after ion milling to the indicated depths: (a) sample 1; (b) sample 2; (c) sample 3; (d) sample 4

3. Comparison of Chemical Bond Intensity

The typical Ti2p XPS curve-fitted spectra of the joint interfaces of the four samples obtained from the Ti side, at an ion-milling depth of 480 nm, are shown in Fig. 7. A comparison of these spectra reveals that the chemical bonds in the four samples are identical. In other words, apart from Ti–O, Ti–C and Ti_2O_3, increasing the laser energy did not create any new chemical bonds. The area under each peak represents the bond intensity. The relative amounts of Ti–O, Ti–C, and Ti_2O_3 in the four samples at various sputtering depths were determined and are presented in Fig. 8. The data show that the intensities of both the Ti–O and Ti–C bonds generated during the joining process increased noticeably with increasing laser energy. Moreover, as the laser input energy increased, the thickness of the interface containing the Ti–O and Ti–C bonds also increased. On the other hand, the energy effect on the intensity of Ti_2O_3 was relatively weak. This suggests that increasing the laser energy mainly promotes the generation of Ti–O and Ti–C bonds to a greater depth at the joint interface. It is understandable that increased laser energy input would raise the temperature in the joint zone to extend the heating time for chemical reaction, which would promote chemical reactions of

the titanium atoms with phenyl carbons and –C=O of the PET chain.

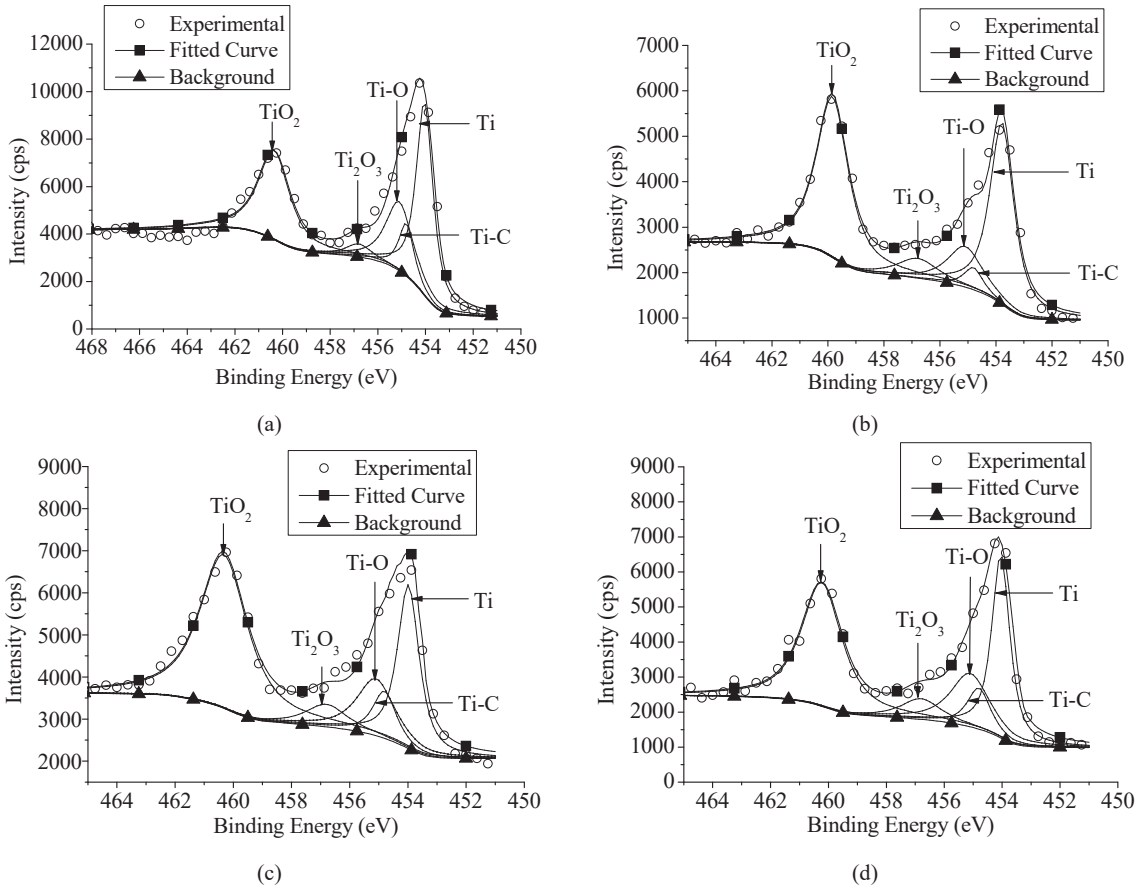

Fig. 7 Typical curve fitting conducted for Ti2p high resolution XPS spectra obtained from the Ti side of the joined samples after ion-milling to the depth of 480 nm: (a) sample 1; (b) sample 2; (c) sample 3; (d) sample 4

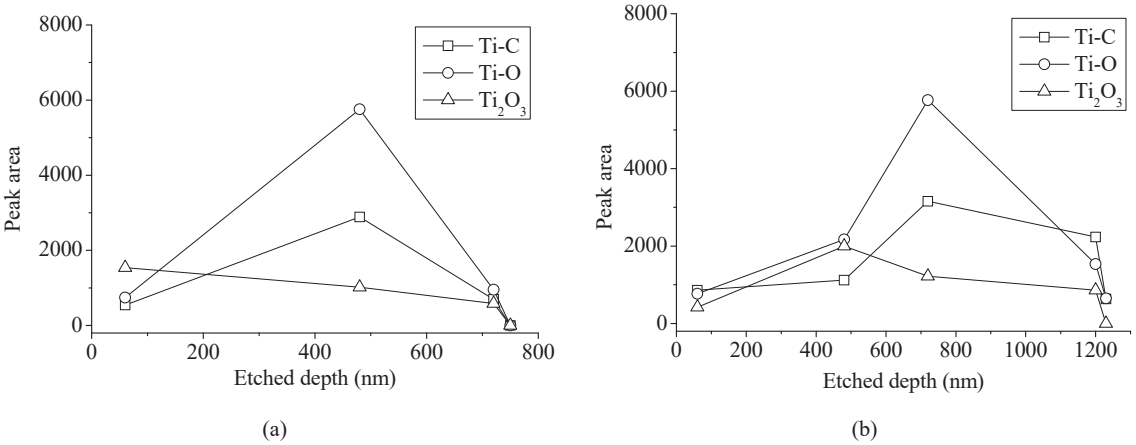

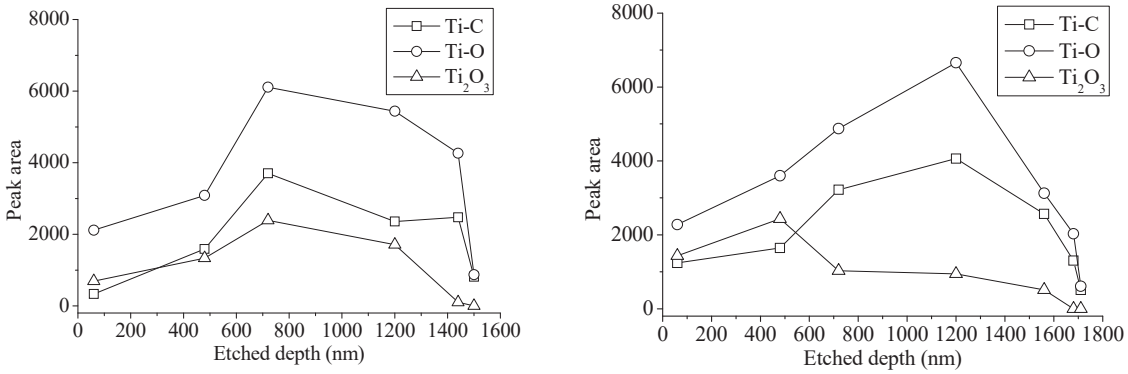

Fig. 8 Areas of the various bond peaks at different etched depths

C. Failure Load

An Instron testing machine was used to measure the failure load of the Ti/PET joined samples produced by using different laser energies at a crosshead speed of 0.5 mm/min. Typical tensile load-displacement curves of the four samples are shown in Fig. 9, with the average failure load presented in Fig. 10. Despite the fact that the amount of porosity in the joint increased as laser energy was increased, the failure load increased from 310 N to 823 N after increasing the laser energy from 1.5 J to 4.5 J. The failure load started to decrease when the laser energy was raised to 6 J. This indicates that although the chemical bonding intensity at the interface was increased as the laser energy was increased, and this should enhance the joint strength, the amount of porosity in the joint also increased. The results thus show that when the amount of bubbles reaches a certain critical value, the weakening effect of the bubbles would outweigh the strengthening effect from a higher chemical bonding intensity. It is also worth noting that although Sample 2 has a slightly lower failure load than Sample 3, the displacement to failure of the former was 66% higher than that of the latter. This indicates that the amount and distribution of porosity has a pronounced effect on ductility.

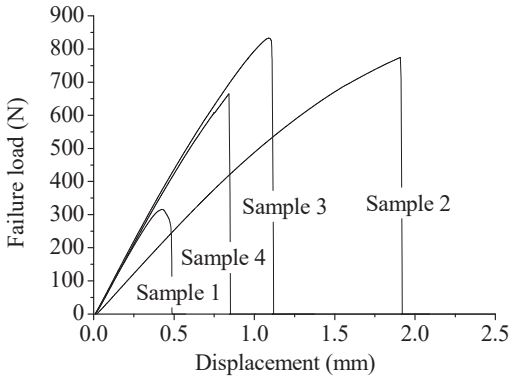

Fig. 9 Typical load-displacement curves of the laser joined samples

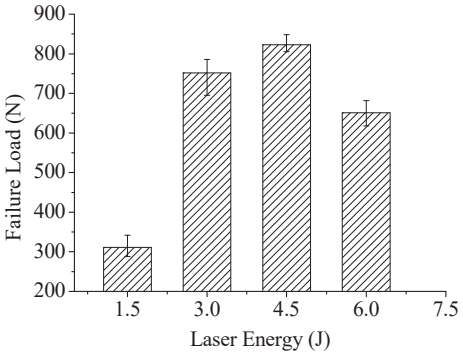

Fig. 10 The effects of laser energy on tensile failure load

IV. Results and Discussion

The effects of laser input energy on the characteristics of the laser-generated bubbles in the weld zone, the intensity of the laser induced chemical bonds at the joint interface and the tensile failure load of the laser joined Ti/PET pairs have been studied. The major findings are summarized below:

a) Laser energy has a significant effect on the amount and distribution of bubbles. A somewhat discrete distribution of bubbles was obtained when a relatively low laser energy was used, which in this study was 3 J. When the energy was raised to 4.5 J, large connected bubbles were formed along the centerline of the weld. Further increase the energy to 6 J, although producing more bubbles, they become more dispersed and occupy a larger area of the weld.

b) The results of the XPS analysis demonstrated that the Ti/PET interface contained new Ti–C, Ti–O and Ti_2O_3 bonds after laser irradiation, and the thickness of the interface, in general, increased with increasing laser energy input. Increasing the laser energy input also increased the intensity count of the chemical bonds.

c) Both the characteristics of the bubbles and the chemical bond intensities of the Ti–C and Ti–O species have pronounced effects on the tensile failure load of the joints. When the amount of bubbles is high, the weakening effect

of the bubbles outweighs the strengthening effect of the high chemical bonding intensity.

Acknowledgment

This research was funded by the Research Committee of the Hong Kong Polytechnic University under research student project account code RTMA.

References

[1] H. L. Gower, R. R. G. M. Pieters, and I. M. Richardson, "Pulsed laser welding of metal-polymer sandwich materials using pulse shaping," Laser Applications, vol. 18, 2006, pp. 35–41.
[2] S. Katayama, and Y. Kawahito, "Laser direct joining of metal and plastic," Scripta Materialia, vol. 59, 2008, pp. 1247–1250.
[3] M. Wahba, Y. Kawahito, and S. Katayama, "Laser direct joining of AZ91D thixomolded Mg alloy and amorphous polyethylene terephthalate," Journal of Materials Processing Technology, vol. 211, 2011, pp. 1166–1174.
[4] Y. Kawahito, Y. Niwa, and S. Katayama, "Laser direct joining between stainless steel and polyethylene terephthalate plastic and reliability evaluation of joints," Welding International, vol. 28, 2004, pp. 107–113.
[5] S. Arai, Y. Kawahito, and S. Katayama, "Effect of surface modification on laser direct joining of cyclic olefin polymer and stainless steel," Materials and Design, vol. 59, 2014, pp. 448–453.
[6] D. G. Georgiev, T. Sultana, A. Mian, G. Auner, H. Herfurth, R. Witte, and G. Newaz, "Laser fabrication and characterization of sub-millimeter joints between polyimide and Ti-coated borosilicate glass," Journal of Materials Science, vol. 40, 2005, pp. 5641–5647.
[7] G. Newaz, A. Mian, T. Sultana, T. Mahmood, D. G. Georgiev, G. Auner, R. Witte, and H. Herfurth, "A comparison between glass/polyimide and titanium/polyimide microjoint performances in cerebrospinal fluid," Journal of Biomedical Materials Research Part A, vol. 79A, 2006, pp. 159–165.
[8] Mian, G. Newaz, T. Mahmood, and G. Auner, "Mechanical characterization of glass/polyimide microjoints fabricated using cw fiber and diode lasers," Journal of Materials Science, vol. 42, 2007, pp. 8150–8157.
[9] Mian, T. Sultana, G. Auner, and G. Newaz, "Bonding mechanisms of laser-fabricated titanium/polyimide and titanium coated glass/polyimide microjoints," Surface and Interface Analysis, vol. 39, pp. 506–511, 2007.
[10] G. L. Georgiev, R. J. Baird, E. F. McCullen, G. Newaz, G. Auner, R. Patwa, and H. Herfurth, "Chemical bond formation during laser bonding of Teflon (R) FEP and titanium," Applied Surface Science, vol. 255, 2009, pp. 7078–7083.
[11] G. and H. Herfurth, "Laser bonding and characterization of Kapton FN/Ti and Teflon FEP/Ti systems," Journal of Materials Science, vol. 44, 2009, pp. 882–888.
[12] T. Sano, S. Iwasaki, Y. Ozeki, K. Itoh, and A. Hirose, "Femtosecond laser direct joining of copper with polyethylene terephthalate," Journal of Materials Transactions, vol. 54, 2013, pp. 926–930.
[13] X. Wang, P. Li, and Z. K. Xu, "Laser transmission joint between PET and titanium for biomedical application," Materials Processing Technology, vol. 210, 2010, pp. 1761–1771.
[14] S. B. Amor, M. Jacquet, P. Fioux, and M. Nardin, "XPS characterisation of plasma treated and zinc oxide coated PET," Applied Surface Science, vol. 255, 2009, pp. 5052–5061.
[15] D. Gonbeau, C. Guimon, G. P. Guillouzo, A. Levasseur, G. Meunier, and R. Dormoy, "XPS study of thin films of titanium oxysulfides," Surface Science, vol. 254, 1991, pp. 81–89.